International Journal of Thermophysics, Vol. 12, No. 5, 1991

Predictive Approach to Thermodynamic Properties of the Metastable Cr_3C Carbide

A. Fernández Guillermet[1]

Received December 21, 1990

In thermodynamic modeling of phase diagrams it is often necessary to deal with the properties of metastable compounds, which are not known from experiments. As an illustrative example, we choose the Cr_3C(oP16) carbide, which is involved in the modeling of the Me_3C(oP16) ("cementite") structure of the Fe–Cr–C system but is metastable in the Cr–C system. We discuss in detail the estimation of its thermodynamic properties, relying on regularities in bonding properties of 3d-transition metal carbides, and an account of the vibrational entropy through the so-called "entropy Debye temperature." Our predictions are compared with values derived in thermodynamic modeling of the Fe–Cr–C phase diagram. Relying on the present results, we perform calculations of metastable phase equilibria in the Cr–C system and use them in analyzing information about Cr_3C from splat-quenching experiments.

KEY WORDS: carbides; chromium compounds; enthalpy; entropy; metastable phases; phase diagrams.

1. INTRODUCTION

1.1. Background

The study of the thermodynamic properties of transition metal alloys and compounds is a subject of great importance in materials science. Accurate thermodynamic information forms the basis of the so-called CALPHAD approach (i.e., the computer coupling of phase diagrams and thermochemistry) to phase stability in alloys. In this approach, pioneered by Kaufman [1, 2], one searches for a consistent description of the thermodynamics of a system, based on modeling the Gibbs energy (G) of

[1] Consejo Nacional de Investigaciones Científicas y Técnicas, Centro Atómico Bariloche, 8400 San Carlos de Bariloche, Argentina.

0195-928X/91/0900-0919$06.50/0

its various phases. The models used in current CALPHAD work are phenomenological and contain parameters which are fitted to selected pieces of experimental information on the phase diagram and thermochemical properties. For stable phases, the necessary information is usually obtained from experiments, but there is often the need for dealing with metastable phases, the properties of which are not known from direct measurements.

1.2. Metastable Compounds in "Two-Sublattice" Modeling

As an important example of situations where information about metastable phases is involved, we may consider the application of the Hillert–Staffansson [3] "two-sublattice" thermodynamic model to carbide phases in ternary and higher-order systems. A system of practical interest is the Fe–Cr–C system, and we choose the modeling of one of its phases, the Me_3C (oP16) (so-called "cementite") phase, to illustrate on the general method applied in this paper. The cementite phase in the Fe–Cr–C system may be represented as $(Fe, Cr)_3C$ and in the two-sublattice model [3] its Gibbs energy per mole of formula units is expressed in terms of three parameters, *viz.*, the Gibbs energy functions of the isomorphous compounds defining the Fe-rich (i.e., "Fe_3C") and Cr-rich (i.e., "Cr_3C") ends of the composition range for $(Fe, Cr)_3C$, and a phenomenological, "regular-solution" type of parameter describing the interaction between atoms of Fe and Cr in the metal sublattice of the carbide phase. The G function of Fe_3C(oP16) has been evaluated from experimental information, e.g., in Ref. 4, but the Gibbs energy of Cr_3C(oP16) is not known. This phase is not stable in the Cr–C system. It has been found in rapidly quenched alloys [5] and its lattice parameters have been determined, but no thermodynamic measurements have been performed. As a consequence, the Gibbs energy function of Cr_3C has previously been treated as an unknown quantity in the modeling of $(Fe, Cr)_3C$, to be determined by searching for the best fit to ternary experimental information, in a so-called "optimization" process. Since the results of such a procedure depend upon the amount and accuracy of the experimental data, it would be useful to have methods for predicting thermodynamic quantities for metastable compounds and judging values from CALPHAD optimizations.

1.3. The Present Study

In the present paper, we discuss how information on the thermodynamics of Cr_3C can be obtained by relying on regularities in bonding properties and vibrational entropy, which have been revealed by recent

work [6] on 3d-transition metal compounds. The present approach has previously [7] been applied to analyzing qualitative information on the possible occurrence of a (cF8) NaCl-structure carbide in the Cr–C system. Here we go a step further and study how the quantitative predictions for Cr_3C compare with the values derived from thermodynamic modeling [8] of the Fe–Cr–C system. Moreover, we study information on the occurrence of the Cr_3C phase in splat-quenched Cr–C alloys [5]. That leads us to an analysis of metastable equilibria in the Cr–C system, using calculations based on our predictions for Cr_3C.

2. THERMODYNAMIC BASIS

The Gibbs energy per mole of formula units of Cr_3C at 101,325 Pa, as a function of T, ${}^0G_m^{Cr_3C}(T)$, is related to the molar enthalpy (${}^0H_m^{Cr_3C}$) and the molar entropy (${}^0S_m^{Cr_3C}$) at the reference temperature $T_0 = 298.15$ K, by integrating the identity

$$\left(\frac{\partial {}^0G_m^{Cr_3C}}{\partial T}\right)_P = -{}^0S_m^{Cr_3C} \tag{1}$$

We obtain

$${}^0G_m^{Cr_3C}(T) = {}^0H_m^{Cr_3C}(T_0) - T_0\,{}^0S_m^{Cr_3C}(T_0) - \int_{T_0}^{T} {}^0S_m^{Cr_3C}(T')\,dT' \tag{2}$$

Next, we follow the convention adopted by the SGTE (Scientific Group Thermodata Europe) organization [9] and refer the ${}^0G_m(T)$ function in Eq. (2) to the weighted sum of the enthalpies of the elements in their stable modifications (i.e., bcc Cr and graphite) at the reference temperature, i.e., to the sum $3\,{}^0H_{Cr}^{bcc}(T_0) + {}^0H_C^{graph}(T_0)$. Subtracting this sum from both sides of Eq. (2) we obtain

$$\begin{aligned} &{}^0G_m^{Cr_3C}(T) - 3\,{}^0H_{Cr}^{bcc}(T_0) - {}^0H_C^{graph}(T_0) \\ &\quad = \Delta\,{}^0H_m^{Cr_3C}(T_0) - T_0\,{}^0S_m^{Cr_3C}(T_0) - \int_{T_0}^{T} {}^0S_m^{Cr_3C}(T')\,dT' \end{aligned} \tag{3}$$

where $\Delta\,{}^0H_m^{Cr_3C}(T_0) \equiv {}^0H_m^{Cr_3C}(T_0) - 3\,{}^0H_{Cr}^{bcc}(T_0) - {}^0H_C^{graph}(T_0)$ is the enthalpy of formation (per mole of formula units) of Cr_3C from the elements in their stable modifications at 298.15 K and 101,325 Pa. Equation (3) summarizes the thermodynamic relations between the properties we focus on in the following when constructing the ${}^0G_m(T_0)$ function for Cr_3C, namely, the enthalpy of formation at $T_0 (= 298.15\ \text{K})$ and the entropy at and above T_0.

3. VIBRATIONAL ENTROPY

The theoretical background of some of the expressions used here may be found, e.g., in Refs. 10 and 11 and in a monograph by Grimvall [12]. Here we give only the main points.

The temperature dependent part of ${}^0G(T)$ is usually dominated by the lattice vibrations, which may be described by a properly defined Debye temperature, θ. Following previous [10, 11] work we use an "entropy Debye temperature," θ_S^0, which is essentially a logarithmic average of the phonon frequencies $\omega(\mathbf{q})$ (when $T > \theta_S$). It is obtained from the $\theta_S(T)$ function which reproduces the experimental vibrational entropy per atom of the compound $[S_{vib}(T)]$ if θ_S is inserted in the Debye model expression S_D for entropy,

$$S_{vib}(T) = S_D[\theta_S(T)/T] \tag{4}$$

At low temperatures ($T \ll \theta_S$), $\theta_S(T)$ varies with T because the true vibrational spectrum is not of the Debye form, and at high temperatures ($T > \theta_S$), it shows a smooth decrease with increasing T, caused by anharmonic softening of the lattice vibrations. To obtain a stable value for θ_S we evaluate θ_S at $T \approx \theta_S$ and denote that θ_S by θ_S^0.

The present predictive approach to high-temperature entropy of a metastable compound relies on constructing a probable $\theta_S(T)$ function. That is made by us in two steps. In the first place we deal with the prediction of the θ_S^0 value and then proceed to account for the decrease in θ_S with increasing T at $T > \theta_S^0$. The prediction of θ_S^0 is based on the use of trends in information on related compounds, but θ_S^0 is not directly suitable for such comparisons because it contains the atomic masses, M. However, in the logarithmically averaged phonon frequency, which is represented by θ_S^0, the masses separate from the interatomic forces [10]. Therefore one can define a quantity k_S, with the dimension of a force constant (i.e., force per length), by

$$\theta_S^0 = (\hbar/k_B)(k_S/M_{eff})^{1/2} \tag{5}$$

Here k_B and $2\pi\hbar$ are Boltzmann's and Planck's constants, respectively, and M_{eff} is the logarithmic average of the vibrating masses. For instance, M_{eff} of Cr_3C is related to the atomic masses of Cr (M_{Cr}) and C (M_C) by

$$M_{eff} = (M_{Cr})^{3/4} \cdot (M_C)^{1/4} \tag{6}$$

The quantity k_S, which contains information on the strength of the average interatomic forces in the compound, has been [10] referred to as the "effective force constant." Previous analyses based on k_S of the

vibrational entropy of the transition metals [13] and their combinations with C, N, and B [10] have revealed remarkable regularities. In the following section we use k_S to construct a quantity with the dimension of energy, which also shows useful regularities and allows the estimation of θ_S^0.

4. TREATMENT OF θ_S^0 AND $\Delta^0 H$

4.1. Systematics of Bonding Properties for Carbides

In Ref. 6 Fernández Guillermet and Grimvall reported an analysis of the bonding properties and the vibrational entropy of a large number of 3d-transition metal carbides with the (cF8) NaCl structure and with complex structures. They studied trends in, i.a., the enthalpy of formation at 298.15 K, and a quantity E_S, with the dimension of energy, defined as

$$E_S(\text{Ry}) = k_S \Omega^{2/3} \tag{7}$$

where Ω is the average volume per atom, which was obtained from the experimental lattice parameters. These properties were found to vary in a regular and related way when studied as a function of the average number of valence electrons per atom ($\text{e} \cdot \text{atom}^{-1}$) in the compound, n_e. A carbide with formula Me_aC_b would have $n_e = (an_{Me} + bn_C)/(a+b)$, where n_{Me} and n_C are the number of valence electrons for atoms Me and C. For C $n_C = 4$ $\text{e} \cdot \text{atom}^{-1}$, and $n_{Me} = 3$ $\text{e} \cdot \text{atom}^{-1}$ for Sc, 4 $\text{e} \cdot \text{atom}^{-1}$ for Ti, 5 $\text{e} \cdot \text{atom}^{-1}$ for V, etc. In Fig. 1, we plot versus n_e the entropy-related characteristic energy E_S(Ry) (Fig. 1a) (1 $\text{Ry} \cdot \text{atom}^{-1} = 1312.8$ $\text{kJ} \cdot \text{mol}^{-1}$) and the (negative) enthalpy of formation (per mol of atoms) at 298.15 K, $-\Delta^0 H$ (Fig. 1b) for 3d-transition metal carbides. By definition, for Cr_3C, $\Delta^0 H = (1/4)\,\Delta^0 H_m^{Cr_3C}(T_0)$. References to the sources of entropy and enthalpy information are given in Ref. 6. Here we briefly comment on the data points representing Me_3C(oP16) compounds (with Me = Mn, Fe, Co, and Ni). The properties of Mn_3C are from an assessment of the experimental information given in Ref. 14. This carbide (data point No. 9) and the other Mn compounds (numbers 7, 8, and 10) fall on the general trend for E_S but not quite so for $-\Delta^0 H$. Such a discrepancy can be related [6] to the properties of α – Mn (i.e., the reference state for $\Delta^0 H$), which shows an anomalously low cohesive energy. The Me_3C(oP16) structure is metastable in the Me–C phase diagram for Me = Fe, Co, and Ni. The properties of Fe_3C(oP16) are, however, known from experiments [4], but for the metastable compounds Co_3C(oP16) and Ni_3C(oP16), we have only indirect information, obtained in CALPHAD analyses of the Fe–Co–C [15] and Fe–Ni–C [16] systems, respectively.

4.2. Predictions for Metastable Carbides

The solid lines in Fig. 1 provide a reasonably good general description of the variation with n_e of two properties related to the strength of the chemical bonding for 3d-transition metal carbides. The left part of the curves ($n_e \leqslant 4.5$ e·atom^{-1}) corresponds to the (cF8) NaCl structure carbides, and the right part ($n_e > 4.5$ e·atom^{-1}) corresponds to complex carbides. The kink shown by the information on the (cF8) NaCl structure is due to varying degree of filling of bonding and antibonding p–d

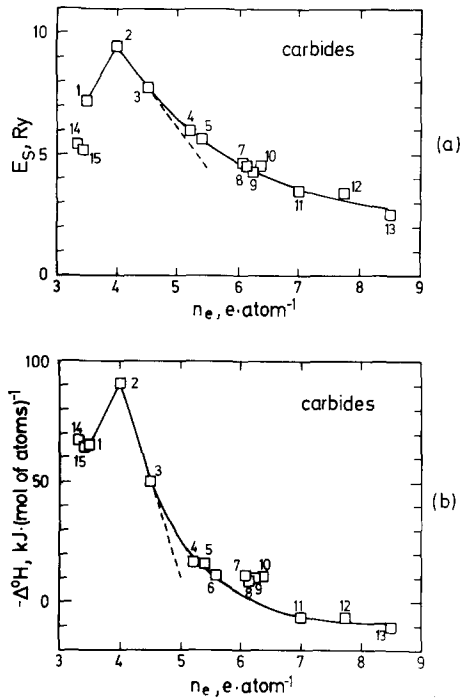

Fig. 1. (a) The entropy-related characteristic energy E_S, defined by Eq. (7), and (b) the negative enthalpy of formation of carbides at 298.15 K ($-\Delta^0 H$), as a function of the average number of valence electrons per atom, n_e. The numbers refer to ScC(1), TiC(2), VC(3), Cr_3C_2(4), Cr_7C_3(5), $Cr_{23}C_6$(6), Mn_7C_3(7), Mn_5C_2(8), Mn_3C(9), $Mn_{23}C_6$(10), Fe_3C(11), Co_3C(12), Ni_3C(13), Sc_2C(14), and Sc_4C_3(15). The dashed lines refer to the (cF8) NaCl structure. From Fernández Guillermet and Grimvall [6].

hybridized electron states, which dominate the interatomic forces [6]. Relying on the lines in Fig. 1 one can estimate the properties of the metastable Cr_3C phase, as follows. From the average number of valence electrons per atom of Cr_3C ($n_e = 5.5$ e · atom^{-1}) and the solid line in Fig. 1a, one estimates E_S. Combination with the experimental [5] volume per atom ($\Omega = 9.966\ 10^{-30}$ m^3 · atom^{-1}) yields k_S (Eq. [7]) and θ_S^0 [Eq. (5)]. In a similar way, from n_e and the solid line in Fig. 1b, one estimates $\Delta^0 H$. In this way one has obtained [6] for the Cr_3C(oP16) phase $\theta_S^0 = 502$ (± 10) K and $\Delta^0 H = -12(\pm 2)$ kJ · (mol of atoms)$^{-1}$.

The study of transition metal carbides has recently [17] been extended to cover binary compounds with formulas MeC, Me_3C_2, Me_2C, Me_7C_3, Me_5C_2, Me_3C, and $Me_{23}C_6$, with Me being Sc, Ti, V, Cr, Mn, Fe, Co, and Ni. Most of those compounds are metastable, but their θ_S^0 and $\Delta^0 H$ have been predicted by applying interpolation and extrapolation procedures, assuming that the bonding properties vary smoothly with n_e. Figure 2, based on the results from Refs. 6, 17, and 18, summarizes

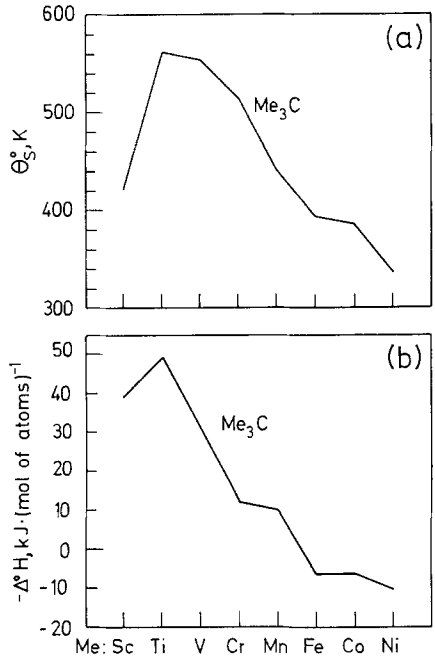

Fig. 2. (a) The entropy Debye temperature θ_S^0 defined in Section 3 and (b) the negative enthalpy of formation ($-\Delta^0 H$) of Me_3C (oP16) compounds, with Me = Sc, Ti, V, Cr, Mn, Fe, Co, and Ni. From Refs. 6, 17, and 18.

the most recent information on θ_S^0 (Fig. 2a) and $\Delta^0 H$ (Fig. 2b) for Me_3C(oP16) 3d-transition metal compounds. It combines results from assessments of thermodynamic data for Mn_3C and Fe_3C [6], with values from CALPHAD analyses for Co_3C and Ni_3C [6], predicted [17] values for Sc_3C, Ti_3C, and Cr_3C, and values for V_3C which were obtained [18] by combining predictions with thermodynamic calculations. The analysis in Ref. 17 led to a new, refined estimate for θ_S^0 of Cr_3C, namely, $\theta_S^0 = 514$ K, which is close to the upper limit of the previous result from Ref. 6 given above. That refined value, together with the result $\Delta^0 H = -12$ kJ · (mol of atoms)$^{-1}$, is the basis of our estimated Gibbs energy function for Cr_3C.

5. TEMPERATURE DEPENDENCE OF θ_S

In line with the considerations in Section 3, we assume that the θ_S^0 value for Cr_3C obtained from the E_S vs n_e correlation corresponds to $T \approx \theta_S^0$ ($=514$ K). At higher temperatures $\theta_S(T)$ is expected to decrease because of anharmonic effects, but a method for predicting the magnitude of the temperature effect upon θ_S has not yet been developed. Hence, we adopt for Cr_3C an approximation suggested in Ref. 7, which is based on comparison with the $\theta_S(T)$ functions for the stable carbides in the Cr–C system. In Fig. 3 we plot, using solid lines, the θ_S versus temperature values

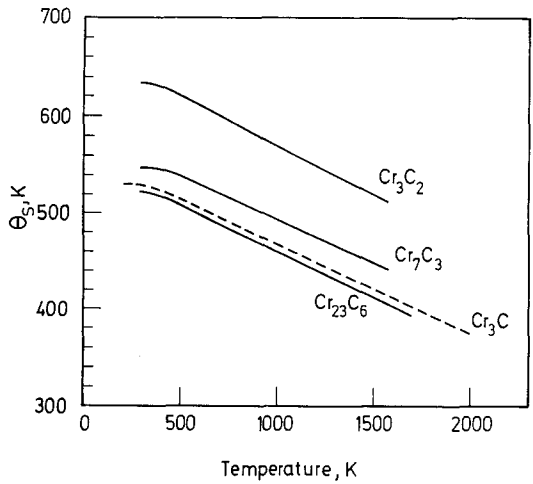

Fig. 3. The θ_S versus T function for Cr_3C_2, Cr_7C_3, and $Cr_{23}C_6$ derived, according to Eq. (4), from entropy values recommended in the JANAF tables [19] (solid lines), and the probable $\theta_S(T)$ function for the metastable Cr_3C carbide constructed in the present work (dashed line).

for the carbides Cr_3C_2, Cr_7C_3, and $Cr_{23}C_6$, derived from the entropy values recommended in the JANAF Tables [19] by applying Eq. (4) and neglecting nonvibrational (e.g., electronic) contributions. A very similar rate of decrease in θ_S with T is observed for the stable carbides, which may now be used to estimate the slope of the θ_S vs T curve for the metastable Cr_3C phase. A probable $\theta_S(T)$ function for Cr_3C is constructed by combining that slope with the condition that $T = \theta_S$ at 514 K (see above). It is represented in Fig. 3 using a dashed line.

6. RESULTS AND DISCUSSION

6.1. Gibbs Energy and Thermodynamic Properties

Once the probable $\theta_S(T)$ function has been established, we approximate the total entropy (per mole of formula units) of Cr_3C, ${}^0S_m^{Cr_3C}(T)$, from the entropy (per mole of atoms) $S_{vib}(T)$, which is obtained from Eq. (4), with $\theta_S(T)$ varying according to the dashed line in Fig. 3, i.e.,

$$ {}^0S_m^{Cr_3C}(T) \simeq 4S_D[\theta_S(T)/T] \tag{8} $$

Next one can insert $\Delta {}^0H_m^{Cr_3C}(T_0)$ from Section 4.2 and ${}^0S_m^{Cr_3C}(T)$ from Eq. (8) in the right-hand side of Eq. (3) and integrate numerically to get values for the quantity ${}^0G_m^{Cr_3C}(T) - 3\,{}^0H_{Cr}^{bcc}(T_0) - {}^0H_C^{graph}(T_0)$. On the other hand, most phase-diagram calculations are performed by adopting a closed expression for the temperature dependence of the Gibbs energy [9]. Therefore we assumed, following recent work on transition metals [20–22], that the Gibbs energy (per mole of formula units) of the metastable Cr_3C phase can be represented by the following expression:

$$ {}^0G_m^{Cr_3C}(T) - 3\,{}^0H_{Cr}^{bcc}(T_0) - {}^0H_C^{graph}(T_0) = a + bT + cT\ln T + dT^{-1} + eT^2 \tag{9} $$

The evaluation of the various parameters was as follows. In the first place we determined the parameters describing the temperature dependence of ${}^0G_m^{Cr_3C}(T)$ (i.e., parameters b, c, d, and e) by fitting to entropy values estimated using Eq. (8) with $\theta_S(T)$ from Fig. 3. Then we determined parameter a from a consideration of the estimated $\Delta {}^0H_m^{Cr_3C}(T_0)$, Section 4.2. The information on the properties of bcc Cr and graphite needed here was taken from Refs. 23 and 24, respectively. All fits reported in the present work were made using PARROT, a computer program for the optimization of thermodynamic model parameters developed by Jansson [25]. The expression for Gibbs energy of Cr_3C arrived at in our work is given in Table I, together with values for various thermodynamic properties.

The present treatment of the temperature dependence of θ_S for the metastable Cr_3C phase of the Cr–C system relies on a comparison with information on the behavior of related phases which are stable in this system. However, there is often the case where such information is not available, and it is interesting to know how large the effect would be of neglecting the variation of θ_S with T. A comparison for Gibbs energy of Cr_3C is given in Fig. 4, where we compare the function (1/4) $[{}^0G_m^{Cr_3C}(T) - 3\,{}^0H_{Cr}^{bcc}(T_0) - H_C^{graph}(T_0)]$ obtained from the descrition in Table I (solid

Table I. Present Description of the Gibbs Energy Versus Temperature Function for the Cr_3C (oP16) Carbide at $P_0 = 101{,}325$ Pa, and Various Thermodynamic Properties[a]

$$298.15\ \text{K} \leqslant T \leqslant 2000\ \text{K}$$

$${}^0G_m^{Cr_3C}(T) - 3\,{}^0H_{Cr}^{bcc}(T_0) - {}^0H_C^{graph}(T_0) = -81{,}785 + 565.22\,T - 94.501\,T\ln T - 1.35426\,10^{-2}\,T^2 + 658{,}998\,T^{-1}$$

$${}^0H_m^{Cr_3C}(T) - 3\,{}^0H_{Cr}^{bcc}(T_0) - {}^0H_C^{graph}(T_0) = -48{,}000\ \text{J}\cdot\text{mol}^{-1}$$

$${}^0H_m^{Cr_3C}(T_0) - {}^0H_m^{Cr_3C}(0) = 14{,}461\ \text{J}\cdot\text{mol}^{-1}$$

T (K)	$C_P(T)$ ($J\cdot K^{-1}\cdot mol^{-1}$)	$H_m(T) - H_m(T_0)$ ($kJ\cdot mol^{-1}$)	$S_m(T) - S_m(0)$ ($J\cdot K^{-1}\cdot mol^{-1}$)	$G_m(T) - 3H_{Cr}^{bcc}(T_0) - H_C^{graph}(T_0)$ ($kJ\cdot mol^{-1}$)
298.15	87.750	0.0000	83.198	−72.791
300.00	87.982	0.1626	83.742	−72.945
400.00	97.098	9.4623	110.43	−82.696
500.00	102.77	19.472	132.75	−94.886
600.00	107.09	29.973	151.88	−109.14
700.00	110.77	40.870	168.67	−125.18
800.00	114.11	52.116	183.68	−142.81
900.00	117.25	63.685	197.30	−161.87
1000.00	120.27	75.562	209.82	−182.24
1100.00	123.21	87.736	221.42	−203.81
1200.00	126.09	100.20	232.26	−226.50
1300.00	128.93	112.95	242.47	−250.24
1400.00	131.75	125.99	252.12	−274.97
1500.00	134.54	139.30	261.31	−300.65
1600.00	137.32	152.89	270.08	−327.22
1700.00	140.09	166.77	278.49	−354.65
1800.00	142.85	180.91	286.57	−382.91
1900.00	145.60	195.33	294.37	−411.96
2000.00	148.34	210.03	301.91	−441.77

[a] The values are given in SI units and correspond to 1 mol of formula units of Cr_3C. Temperature values according to IPTS68. $T_0 = 298.15$ K. The properties of bcc Cr and graphite according to Refs. 23 and 24, respectively.

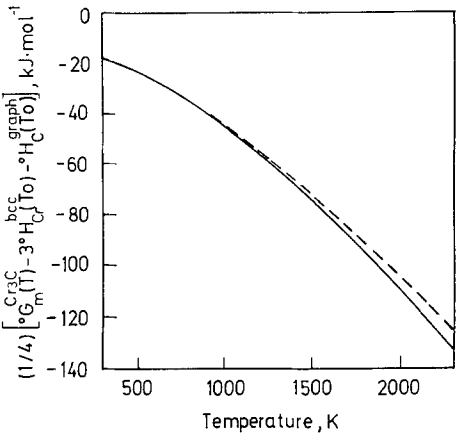

Fig. 4. The quantity $(1/4)[{}^0G_m^{Cr_3C}(T) - 3\,{}^0H_{Cr}^{bcc}(T_0) - {}^0H_C^{graph}(T_0)]$, defined by Eq. (3), according to the description in Table I (solid line), and a calculation based on the approximation $\theta_S = 514$ K (dashed line); see text.

line), with that obtained if Eq. (9) is fitted to entropy values according to the approximation $\theta_S(T) = \theta_S^0$ ($= 514$ K) (dashed line). It is evident that the effect of the approximation upon ${}^0G_m^{Cr_3C}(T)$ is relatively small up to about 1000 K but increases with T. For instance, at 2000 K that approximation would lead to overestimating ${}^0G$ by 5.4 kJ · (mol of atoms)$^{-1}$. It is also interesting to relate that error in ${}^0G$ with those one makes in ${}^0H$ and in ${}^0S$ when taking $\theta_S(T) = 514$ K. We find that at 2000 K, ${}^0H$ and ${}^0S$ would be underestimated by 10.6 kJ · (mol of atoms)$^{-1}$ and 8 J · K^{-1} · (mol of atoms)$^{-1}$, respectively. Because the changes in ${}^0H$ and in ${}^0S$ partially cancel in ${}^0G$ ($= {}^0H - T\,{}^0S$), the magnitude of the error in Gibbs energy [i.e., 5.4 kJ · (mol of atoms)$^{-1}$] is smaller than that in enthalpy [i.e., 10.6 kJ · (mol of atoms)$^{-1}$]. A further consideration of the effect of neglecting the temperature dependence of θ_S is made when analyzing metastable equilibria in the Cr–C system, in Section 7.

6.2. Comparison with Results from CALPHAD Work

Another question of interest in connection with the use of predicted Gibbs energies is how the values obtained here compare with those derived in a CALPHAD analysis of the $(Fe, Cr)_3C$ phase in the Fe–Cr–C system. Here we compare with the results of the recent analysis by Andersson [8].

His treatment was based on assuming a linear expression for the Gibbs energy of formation of Cr_3C from bcc Cr and graphite, i.e.,

$$^{0}G_{m}^{Cr_3C}(T) = 3\,^{0}G_{Cr}^{bcc}(T) + {}^{0}G_{C}^{graph}(T) + h + sT \qquad (10)$$

where the constants h and s were treated by him as adjustable parameters in a fit to experimental data. He analyzed information on the equilibrium distribution of Cr between the $(Fe, Cr)_3C$ carbide and the bcc or fcc phase, which was available for temperatures between 773 and 1043 K (cf. Ref. 8). A comparison with the present results in that temperature range is given in Fig. 5. In Fig. 5a we plot the difference ΔG^* [in kJ·(mol of atoms)$^{-1}$]

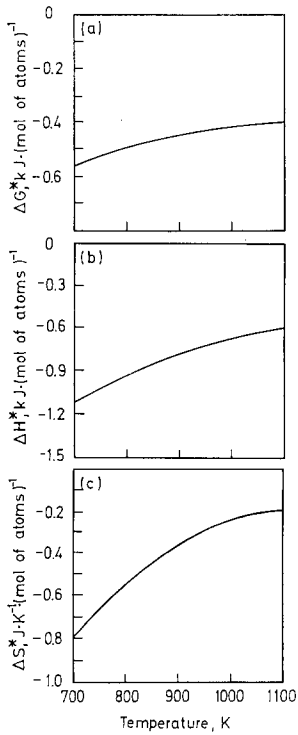

Fig. 5. The difference in (a) Gibbs energy, (b) enthalpy, and (c) entropy values, between the present thermodynamic description for Cr_3C (Table I) and hat derived by Andersson [8] from thermodynamic modeling of the Fe–Cr–C phase diagram.

between the Gibbs energy values according to the description in Table I and that obtained by Andersson [8]. The ${}^0G$ values according to his parameters are, in that range, larger than ours, but the discrepancy [less than 0.6 kJ · (mol of atoms)$^{-1}$] is small, and we take Fig. 5a as indicating a good agreement between our predicted Gibbs energies and those derived by Andersson [8]. His analysis of the $(Fe, Cr)_3C$ carbide relied heavily on phase diagram data, which give information on Gibbs energies, but no enthalpy or entropy information on Cr_3C was available. On the other hand, the "linear Gibbs energy of formation approximation" [Eq. (10)] is frequently used in CALPHAD analyses and one would like to know how the enthalpy and entropy values extracted from the fit based on Eq. (10) compare with our predictions. The differences between our and his enthalpy values (ΔH^*) and entropy values (ΔS^*), expressed per mole of atoms, are given in Figs. 5b and c, respectively. These comparisons indicate that the differences in ${}^0H$ and ${}^0S$ are not large in the temperature range where the fit was made. If the comparison is made on a wider temperature range, the discrepancies on ${}^0H$ and ${}^0S$ increase, which is natural, considering that the heat capacity at constant pressure (C_P) of Cr_3C is not treated here as in Ref. 8. Equation (10) assumes that C_P for Cr_3C can be expressed as the weighted sum of C_P for bcc Cr and graphite, i.e., the so-called Neumann–Kopp approximation. Such an approximation is not involved in the present treatment, which relies on the temperature dependence of the entropy expected from a consideration of θ_S for related compounds (Fig. 3), and thus it is expected to give more realistic values of ${}^0H$ and ${}^0S$. However, due to the partial cancellation of the errors in ${}^0H$ and ${}^0S$ (cf. Section 6.1), the magnitude of the discrepancy in ${}^0G$ between the present description (Table I) and the extrapolations based on Eq. (10) remains reasonably small, *viz.*, less than 1.5 kJ · (mol of atoms)$^{-1}$ for temperatures between 300 and 2300 K. This suggests a reasonably good agreement between our and his ${}^0G$ values over the temperature range of most practical interest.

7. APPLICATION: ANALYSIS OF METASTABLE PHASE EQUILIBRIA IN THE Cr–C SYSTEM

7.1. Thermodynamic Predictions for Cr–C Alloys

The study of phase equilibrium referred to in Section 6 concerns the ternary Fe–Cr–C system [8]. Now we turn to the binary Cr–C system. The thermodynamic properties of the stable solution phases (bcc and liquid) and stable carbides ($Cr_{23}C_6$, Cr_7C_3, Cr_3C_2) and the stable phase diagram have been evaluated by Andersson [26] using binary experimental information and adopting the descriptions of Cr [23] and graphite [24]

referred to in Section 6.1. The Cr_3C carbide is not a stable phase in the system, but it has been obtained in splat-quenching experiments by Inoue and Masumoto [5]. They studied binary Cr–C alloys with a carbon content up to $x_C = 0.30$, where x_C denotes the mole fraction of C. In Fig. 6 we compare the constitution of the rapidly quenched alloys according to Ref. 5 (upper part) with the stable Cr–C phase diagram (lower part) calculated using the thermodynamic descrition by Andersson [26]. All phase-diagram calculations reported by us were made using the Thermo-Calc system [27]. It is evident that the constitution of the as-quenched alloys with $x_C \leqslant 0.13$ (i.e., "bcc + $Cr_{23}C_6$") and $x_C \geqslant 0.22$ (i.e., "$Cr_{23}C_6$ + Cr_7C_3") can be accounted for by the stable phase diagram, in spite of rapid quenching from the melt. These alloys are not discussed further. Contrasting with that, quenched alloys with $0.13 < x_C < 0.22$ showed a two-phase state of bcc + Cr_3C, whereas the phase diagram in Fig. 6 indicates that the stable two-phase states for solid alloys in that composition range are bcc + $Cr_{23}C_6$ (if $0.13 < x_C < 0.21$) and $Cr_{23}C_6 + Cr_7C_3$ (if $0.21 < x_C$).

The reason why neither $Cr_{23}C_6$ nor Cr_7C_3 was formed in that group of alloys is not known, and Inoue and Masumoto [5] discussed the factors

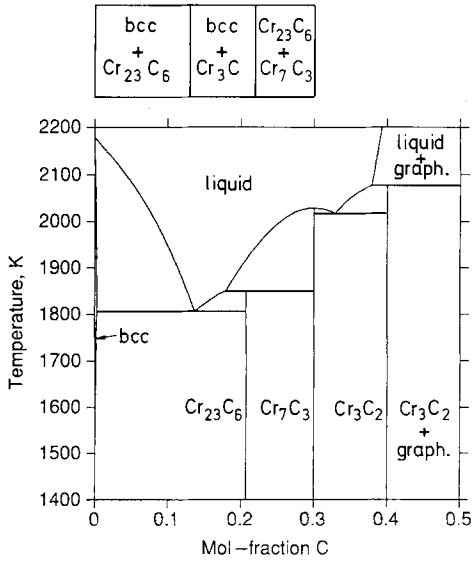

Fig. 6. Lower: The stable Cr–C phase diagram calculated using the thermodynamic description assessed by Andersson [26]. Upper: The constitution of rapidly quenched Cr–C alloys, according to Inoue and Masumoto [5].

that could have affected the nucleation of these carbides from the melt. That concerns the kinetics, but in analyzing the formation of metastable phases, thermodynamic considerations have also been useful (cf., e.g., the study of a metastable Cr–Ni phase in Ref. 28). As a first step in the analysis of the present case, it would, for instance, be useful to know the equilibrium constitution for solid alloys with $0.13 < x_C < 0.22$, if one assumes that, by some (unknown) reason, the stable phases $Cr_{23}C_6$ and Cr_7C_3 do not form. We studied this question by performing a calculation of the Cr–C phase diagram where Cr_3C was included as one of the competing phases, with properties according to Table I, but $Cr_{23}C_6$ and Cr_7C_3 were excluded, and the other phases in the system (i.e., bcc, liquid, Cr_3C_2, and graphite) were treated as in the calculation in Fig. 6. The calculated metastable Cr–C phase diagram is presented in Fig. 7. We also indicate, using vertical dashed lines, the composition limits $x_C = 0.13$ and $x_C = 0.22$. Our calculation predicts that in the absence of $Cr_{23}C_6$ and Cr_7C_3, the equilibrium constitu-

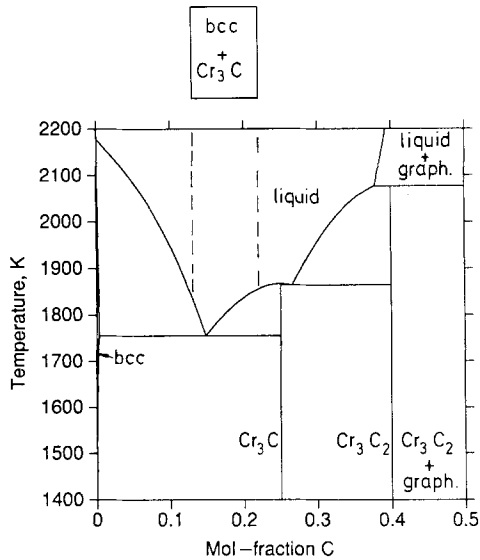

Fig. 7. Lower: The metastable Cr–C phase diagram calculated under the assumption that the stable carbides $Cr_{23}C_6$ and Cr_7C_3 do not form. In this calculation Cr_3C is described according to Table I, and the other phases are treated as in Fig. 6. The dashed lines are to guide the eye. Upper: The constitution of the rapidly quenched Cr–C alloys with carbon contents (in mole fraction) between 0.13 and 0.22, according to Inoue and Masumoto [5].

tion of solid alloys with $0.13 < x_C < 0.22$ will be a two-phase state of bcc + Cr_3C. This thermodynamic prediction accounts for the constitution observed in the quenched alloys from Ref. 5. Since one may ask how sensitive this prediction is to the present extrapolation procedure for high-temperature properties of Cr_3C, we performed a new calculation for the hypothetical case where one completely neglects the temperature dependence of $\theta_S(T)$. The calculated phase diagram is given in Fig. 8. Compared with the previous result (Fig. 7), the phase diagram in Fig. 8 shows the changes reflecting the underestimation of the high-temperature stability of Cr_3C, which was expected from the comparison in Fig. 4. However, in spite of these changes, the calculation in Fig. 8 leads to the same thermodynamic prediction, which accounts for the observations in Ref. 5.

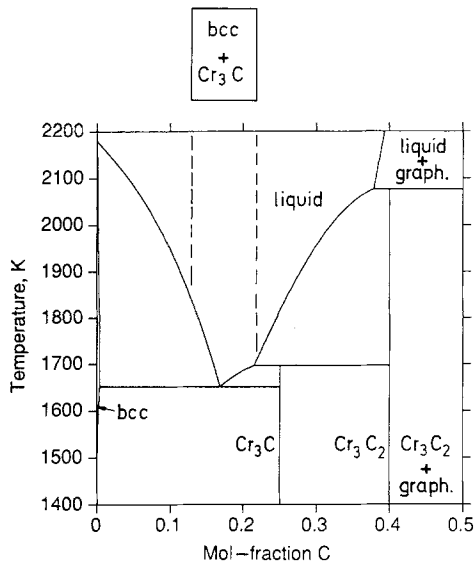

Fig. 8. Lower: The metastable Cr–C phase diagram calculated under the assumption that the stable carbides $Cr_{23}C_6$ and Cr_7C_3 do not form. In this calculation Cr_3C is given properties according to the approximation $\theta_S = 514$ K, (see text), and the other phases are treated as in Figs. 6 and 7. The dashed lines are to guide the eye. Upper: The constitution of the rapidly quenched Cr–C alloys with carbon contents (in mole fraction) between 0.13 and 0.22, according to Inoue and Masumoto [5].

7.2. Predicted Melting Temperature for Cr_3C

Information on melting temperature (T_f) of metastable phases plays a key role in the so-called CALPHAD approach to phase stabilities [1, 29]. There are also empirical approaches such as the well-known Lindemann formula, which has been used [30, 31] to estimate Debye temperatures from T_f. In the present analysis no assumption was made about the melting temperature for Cr_3C. This quantity was, instead, obtained here from a thermodynamic calculation, where the Gibbs energy of Cr_3C is described according to Table I, and the liquid phase according to Ref. 8. The result is $T_f = 1867$ K, which is the temperature of congruent melting of Cr_3C in the metastable phase diagram in Fig. 7. For comparison, we repeat the calculation neglecting the temperature dependence of θ_S, and obtain 1708 K. This corresponds to an underestimation of T_f of about 0.09 T_f and would imply a congruent melting point for Cr_3C which is metastable with respect to the liquid + Cr_3C_2 two-phase equilibrium (Fig. 8).

8. SUMMARY AND CONCLUDING REMARKS

In thermodynamic modeling of alloy systems, it is often necessary to deal with metastable phases, which are not known from experiments, and there is a need for estimation methods which can serve as a complement of the CALPHAD optimization techniques. A possible approach to this problem has been applied here. It relies on a systematics of bonding properties for 3d-transition metal compounds and the properties of the so-called entropy Debye temperature. We choose the Cr_3C carbide as a representative example of a large group of metastable compounds, which are involved in the application of the two-sublattice thermodynamic model to ternary and higher-order carbide systems, and estimate its thermodynamics properties. We find that our predictions are consistent with information derived in CALPHAD work and that one can use our results to account for observations on the formation of Cr_3C in Cr–C alloys.

ACKNOWLEDGMENTS

It is a pleasure to acknowledge many discussions with Professor Göran Grimvall. I also like to thank Professor Mats Hillert and Dr. Larry Kaufman for stimulating discussions on the lattice-stability problem and for their continuous interest in my work.

REFERENCES

1. L. Kaufman and H. Bernstein, *Computer Calculation of Phase Diagrams* (Academic Press, New York, 1970).

2. Cf. the *CALPHAD Journal*, Pergamon Press, New York.
3. M. Hillert and L.-I. Staffansson, *Acta Chem. Scand.* **24**:3618 (1970).
4. P. Gustafson, *Scand. J. Metall.* **14**:259 (1985).
5. A. Inoue and T. Masumoto, *Scripta Metall.* **13**:711 (1979).
6. A. Fernández Guillermet and G. Grimvall, *Phys. Rev.* **B40**:10582 (1989).
7. A. Fernández Guillermet and G. Grimvall, *Z. Metallkunde* **81**:521 (1990).
8. J.-O. Andersson, *Metall. Trans.* **19A**:627 (1988).
9. M. Hillert, in *Computer Modeling of Phase Diagrams*, L.H. Bennett, ed. (The Metallurgical Society, Warrendale, 1986).
10. G. Grimvall and J. Rosén, *Int. J. Thermophys.* **4**:139 (1983).
11. J. Rosén and G. Grimvall, *Phys. Rev.* **B27**:7199 (1983).
12. G. Grimvall, *Thermophysical Properties of Materials* (North-Holland, Amsterdam, 1986).
13. A. Fernández Guillermet and G. Grimvall, *Phys. Rev.* **B40**:1521 (1989).
14. W. Huang, *Scand. J. Metall.* **19**:26 (1990).
15. A. Fernández Guillermet, *Z. Metallkunde* **79**:317 (1988).
16. A. Gabriel, P. Gustafson, and I. Ansara, *CALPHAD* **11**:203 (1987).
17. A. Fernández Guillermet and G. Grimvall, Report TRITA-MAC-0447 (Royal Institute of Technology, Stockholm, Sweden, 1990).
18. A. Fernández Guillermet and W. Huang, Report TRITA-MAC-0440 (Royal Institute of Technology, Stockholm, Sweden, 1990).
19. *JANAF Thermochemical Tables*, 3rd ed., M. W. Chase, C. A. Davies, J. R. Downey, Jr., D. J. Frurip, R. A. McDonald, and A. N. Syverud, eds., *J. Phys. Chem. Ref. Data* **14**:Suppl. 1 (1985).
20. A. Fernández Guillermet and W. Huang, *Int. J. Thermophys.* **11**:949 (1990).
21. A. Fernández Guillermet and G. Grimvall, *J. Less-Common Metals* **147**:195 (1989).
22. A. Fernández Guillermet, *High Temp.-High Press.* **19**:119 (1987).
23. J.-O. Andersson, *Int. J. Thermophys.* **6**:411 (1985).
24. P. Gustafson, *Carbon* **24**:169 (1986).
25. B. Jansson, Ph.D. thesis (Dept. Phys. Met., Royal Institute of Technology, Stockholm, Sweden, 1984).
26. J.-O. Andersson, *CALPHAD* **11**:271 (1987).
27. B. Sundman, B. Jansson, and J.-O. Andersson, *CALPHAD* **9**:153 (1985).
28. M. Kikuchi, A. Fernández Guillermet, M. Hillert, G. Cliff, and G. W. Lorimer, *Acta Metall. Mater.* **38**:165 (1990).
29. A. Fernández Guillermet and M. Hillert, *CALPHAD* **12**:337 (1988).
30. K. A. Gschneider, in *Solid State Physics*, F. Seitz and D. Turnbull, eds. (Academic, New York, 1964), Vol. 16, p. 275.
31. L. Kaufman, *Trans. AIME* **224**:1006 (1962).